Preparation, characterization and adsorption activity of highly porous metal-organic framework; MOF-199

S A.El-Hakam, A. M Youssef, M M Kaid

Department of Chemistry, Faculty of Science, Mansoura University,

Mansoura, P.O.Box 70, Mansoura- Egypt

* Correspondence to: Mahmoud Mohammed Kaid, E-mail: MahmoudKaid@mans.edu.eg or MahmoudKaid1@gmail.com. Phone: 01007575797

Abstract: This paper reports an effective approach for synthesis of MOF-199 through solvothermal method. The synthesized MOF-199 was characterized by sets of different techniques such as FT-IR, and SEM and applied successfully for adsorption of methylene blue dye from simulated aqueous solution. The FT-IR results indicated that MOF-199 was indeed synthesized and SEM confirmed that a crystalline framework was completely achieved and matched the fully octahedral shape. To understand adsorption fairly, the effects of initial dye concentration, pH of solution, adsorbent dosage, contact time and temperature on the adsorption process were studied. Kinetic studies, in addition, the two familiar isotherms; Langmuir and Freundlich models were also reported to determine the adsorption characteristics. The results of Adsorption experiments displayed that the adsorption kinetic and isotherms fitted well with pseudo 2nd order and Langmuir model, respectively. The maximum uptake capacity of MB at 25°C was found to be 103.5 mg.g^{-1} and even after the 5th run durability, the uptake capacity reduced only within 5%, proving that the framework of MOF-199 has good stability

Introduction:

Metal organic frameworks (MOFs) are class of porous materials that constructed by mixing of metal ions (SBUs) and organic linker creating crystalline framework with permanent porosity [1–3]. MOFs have gained unusual attention in the early 1990's with the popularization of the crystal engineering concept. Their scientific interest has been specially multiplied in accordance with the pioneering works of Yaghi [4], Williams [3] and Kitagawa [5]. During the last two decades, the citations and publications of MOFs witnessed an exponentially rise with more than 28,000 various MOFs being synthesized and potentially applied in different fields [6].

The flexibility of MOFs is based on numerous factors involving the nature of organic linkers, pore geometry, secondary building units (SBUs) and solvent molecules

[7]. Accurate selection of MOFs components can produce an ultrahigh porous crystal with high chemical and thermal stability. The thermal stability of MOFs ranges from 250°C to 500°C due to the strong bonds formed within the MOFs (e.g., M-O, C-C, C-H, and C-O) [11–14]. Chemically stable MOFs has been a challenge because of their tendency to link-displacement reactions when they treated with solvents over prolonged periods of time (days). The first example of an exceptional chemically stable MOF is zeolitic imidazolate framework-8 [ZIF-8, Zn(MIm)$_2$], which was reported in 2006 [12]. ZIF-8 is unchanged after immersion in concentrated sodium hydroxide for 24 hours at 100°C and in benzene, boiling methanol, and water for 7 days. MOFs based on Zr(IV) offer high chemical stability; UiO-66 [Zr$_6$O$_4$(OH)$_4$(BDC)$_6$] and its Br- and NO$_2$-functionalized derivatives show high base

(NaOH, pH = 14) and acid resistance (HCl, pH = 1) [13,14].

Along these lines, the multilateral physico-chemical properties of MOFs (simple design, easy operation and reusability, easily modifiable structure, permanent porosity, topology, crystalline nature, thermal/chemical stability and tunable band gaps) made these materials good candidates for fuels storage (hydrogen and methane), gas storage and separation, biomedical imaging, catalysis applications, and proton, electron, and ion conduction, to mention a few [7–10,15].

Water is all-important for life as one of the most indispensable natural resources [16–18]. Water contamination has become a critical worldwide case with the fast-growing of modern industry and the increase of human activities [19,20]. The organic contaminants species in wastewater involving pesticide, poly aromatic hydrocarbons, pharmaceuticals, agrochemicals, dyes and so forth are more diversified, richer and mainly are highly toxic, causing non-negligible environmental threats and serious illness [21–23].

Numerous pioneering techniques and methods have been progressed in WWT through various technologies involving separation processing, filtration, coagulation, chemical precipitation, bioremediation and photocatalytic oxidation [24–27]. In spite of that, the application of these approaches and strategies in WWT are not perfect and still has many technical restrictions such as high energy requirements, lower economic benefit, operational difficulties (demand of space-consuming facilities and complex instruments with high maintenance costs) and inefficiency [28]. Contrariwise, Adsorption technique can eliminate hazardous materials and contaminants from wastewater at lower temperature and energy [29].

Based on the statistics, many tons of synthetic dyes are released annually into water [30]. For MOFs, there are many factors affects the adsorptive elimination of dye pollutants in aqueous environments, including the surface wettability, the sample sizes, the type of adsorbed dye and so on [1,31].

In this paper, we introduced an effective approach for preparation of ultra-highly porous

MOF-199 well Known as HKUST-1 achieved by a conventional solvothermal method. This work offers MOF-199 with numerous advantages such as straightforward synthetic route, high thermal and chemical stability, simple recovery without losing its efficiency which makes it green and efficient adsorbent. Applications of MOF-199 in the adsorptive removal of organic pollutants were examined by studying the uptake of methylene blue (MB) dye.

2. Materials and methods

2. 1. Materials

1,3,5-tricarboxylic acid benzene (H$_3$BTC) and CuCL$_2$.2H$_2$O used as organic linker and SBUs, respectively, were supplied from Alfa-Aeser Co. Methylene blue was supplied from Sigma-Aldrich chemicals Co. N, N-dimethylformamide "DMF" and ethanol are with analytical grades and were used as solvent without any further purification. Deionized water used through whole experiments.

2. 2. Preparation of MOF-199

In a typical case, deep purple crystals of MOF-199 were synthesized by solvothermal method as previously reported [1]. In brief, 1.234 g of CuCl$_2$.2H$_2$O and 0.9414 g of H$_3$BTC were dissolved in a mixture of dist. water, DMF and ethanol (8:12:16 ml, respectively). After vigorous stirring for about 0.5h at RT, the homogenous solution was transferred into Teflon-lined autoclave and thermally treated at 85°C in an isothermal furnace for 24 hours. The resultant product was filtered using centrifuge, washed with DMF and ethanol several times and finally, dried at 80°C under vacuum for 6h.

2. 3. Adsorption study

Stock solution of methylene blue (1000 mg/l) was prepared by dissolving 1g solid MB in 1L dist. Water. The working solutions (25-300 mg/L) of MB was prepared by diluting the stock solution with H$_2$O. Stock solutions of MB (between 1 and 10 mg/L) were used to investigate the calibration curves of absorbance and the maximum wavelength (λ_{max}) was found to be 665 nm for MB dye. Adsorption studies were performed with 50 mg of MOF-199 as adsorbent, 50 mL of MB solution with initial concentration between 25-300 mg/l. The pH of MB was adjusted carefully between 2 and 12 to

demonstrate its influence on MB uptake, using 0.1M NaOH and 0.1M HCl. After the contact time of adsorption, MB solution was separated from the adsorbent using centrifuge and the remaining concentration of MB was investigated from the following equation: $q_e = \frac{[(C_0 - C_e)V]}{m}$

Where q_e is the adsorbent capacity at equilibrium; C_0 and C_e are the dye concentration (initial and equilibrium, respectively) , V is the volume of the working solution in liter and m is the adsorbent mass in gram [29]. The kinetic study was performed using 50 mL MB dye solution with various initial concentrations, 50 mg adsorbent, pH 10, for 24 h at different ambient temperatures of 25, 35, 45 and 60°C (to investigate the temperature effect in the removal of MB and MG from aqueous media).

2. 3. Characterization

The as-synthesized MOF-199 was characterized using different techniques. FT-IR analysis has been recorded on a MATTSON FT-IR-5000S spectrophotometer using a KBr pellets and used effectively in proving the successful preparation of MOF-199. The bulk crystallinity of MOF-199 was obtained using scanning electron microscope (Jeol JSM-6510).

3. Results and discussion

3. 1. Characterization of MOF-199

3. 1. 1. FT-IR spectroscopy

Fig. 1A exhibits FT-IR spectral analysis of the as-prepared MOF-199. The strong absorption peak at 1640 cm^{-1} in conjunction with the disappearance of strong peaks at 1760–1690 cm^{-1} approved the deprotonation of carboxyl groups (–COOH) in 1,3,5-benzenetricarboxylate upon the interaction with Cupper ions [32,34] confirming the formation of MOF which also proved by the softy peaks around 480 and 730 cm^{-1} spectral range that mainly due to the in plane and out plane bending modes of (COO^{-1}) carboxylate group [35]. The sharp peaks around 767 cm^{-1} and between 1380 – 1600 cm^{-1} related to C-H bending vibrations and C=C stretching vibration of benzene ring, respectively [34]; indicating the presence of H$_3$BTC linker (organic ligand) in the synthesized MOF. The moderate peak at 727 cm^{-1} featured for the

(Cu–O) vibration mode, indicated that MOF-199 was indeed synthesized. The broad peaks in the spectral domain of 3000–3600 likely because of the acidic OH of carboxyl (-COOH) group or crystalline water.

3. 1. 2. Morphology of MOF-199

SEM micrograph for MOF-199 confirmed that a crystalline framework was completely achieved and matched the fully octahedral shape with a relatively rough surface (Fig. 1B).
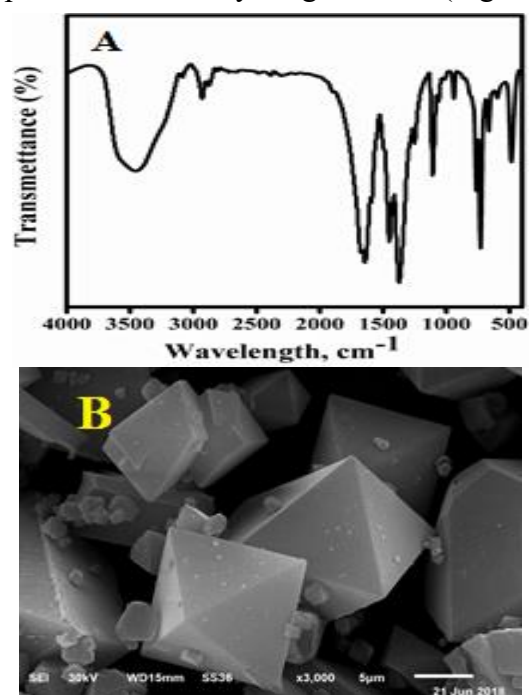
Fig. (1): (A) FT-IR spectroscopy and (B) SEM micrographs of HKUST-1

3. 2. Adsorption activity

MOF-199 was successfully applied in adsorption of MB which usually present in positive form. That is may be due to the electrostatic attraction between negatively charged of the adsorbent surface and the cationic dye, in addition to the N in MB dye structure can form a hydrogen bond with the H on carboxyl groups of MOF-199.

3. 2. 1. Detection of single operating parameter effects the adsorptive uptake of MB using MOF-199

The individual effects of solution pH, adsorption time, initial dye concentration, adsorbent dose and temperature on the uptake efficiency of MB dye using MOF-199 was studied to determine the optimal conditions. In order to attain that, we detect the influence resulted by changes in a single operating parameter while the others were maintained

constant. The optimum value and the studied range of each parameter for removal of MB dye by MOF-199 were recorded at Table 1. under optimum conditions, MOF-199 exhibited maximum uptake efficiency (90%) from 75 mg/l of MB dye.

Table (1): Detection the optimum value of each parameter for MB dye adsorption using MOF-199.

Operating parameter	Test rang	Optimum value
pH	2-12	10
Contact time (h)	0-24	8
Adsorbent dosage (g)	0.01-0.09	0.05
Initial dye concentration (mg/L)	25-300	75
Temperature (^{o}C)	25-60	25

3. 2. 1. 1. Solution pH

It is well-known that pH has a great influence on ionization degree of the adsorptive dye, as well the charge of the adsorbent surface [36]. MB as a cationic dye gets protonated in the acidic media while deprotonated at higher pH. According to above, the pH has a significant role in the removal of MB dye. MOF-199 adsorbent applied in MB removal has numerous carboxyl groups which act as active sites and responsible for MB adsorption uptake. A series of MB bottles with pH varying from 2 to 12 was prepared as a batch experiment. The results showed that MB dye adsorption increased linearly from (16.8 mg/g) at pH 2 to reach maximum (67.7 mg/g) around pH 10 as shown in Fig. 2A. That's may be due to at lower pH (2-4) i.e. higher hydrogen concentrations, H_3O^+ inhibits the approval of MB cations and hence MB uptake was decreased. As the pH quite increases, the competition of H_3O^+ ions with dye cation reduced and the carboxyl groups of MOF-199 adsorbent become more negatively charged and led to better electrostatic attraction [36,37].

3. 2. 1. 2. Contact time

The influence of contact time was conducted for a period of 24 hours. It was observed that the uptake of MB dye onto MOF-199 was very rapid initially, then increased gradually till achieves equilibrium with the prolongation of time contact as shown in Fig. 2B. Based on these results, 8h was taken as the equilibrium time for MB dye adsorption. At the beginning of adsorption, binding (active) sites of adsorbent were freely available to bind adsorbate, which saturated as time proceeds.

The exhausted binding sites after saturation repels the coming adsorbates, also the concentration gradient between the solution and solid surface has been changed [36–38]. Previously studies also have been reported that with the time proceeds the adsorption may decrease due to partial coverage of the adsorbent active sites [38–44].

3. 2. 1. 3. Initial dye concentration

We studied the MB initial dye concentration in the range of 25 to 300 mg/l. It was observed that the adsorption capacity at equilibrium (q_e) increases by increasing the initial dye concentration. The adsorption efficiency has been reached closely 100% at lower initial concentration (25, 50 mg/l), then decreased at higher concentration (200 mg/L) to 50% as shown in Fig. 2C. Dye adsorption efficiency was significantly higher for lower initial concentration due to plenty of freely active sites on the adsorbent surface which has been saturated at extremely higher dye concentration and as a result the adsorption slowed down due to the competition between ions for the available binding sites [38–42].
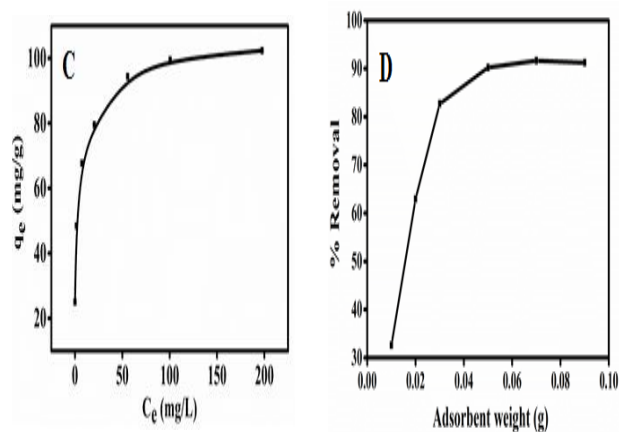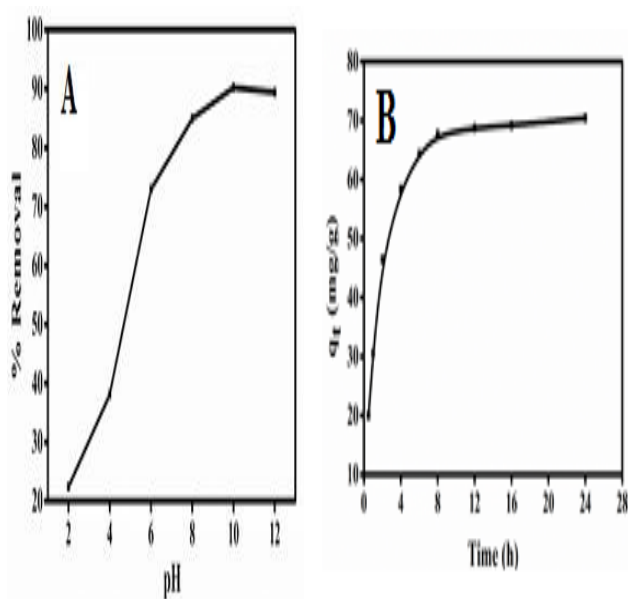
3. 2. 1. 4. Adsorbent dose

The effect of MOF-199 weight was studied in the range of 0.01-0.1 g/ml solution. The study shows that the adsorption of MB dye increases when MOF-199 weight increased and the maximum dye adsorption furnished with 0.05 g adsorbent dose as shown in Fig. 2D. After 0.07 mg, the adsorption slightly decreased again which may be due to adsorbent aggregation and resultantly, the surface area, the availability of active sites and the adsorption efficiency are decreased [44–47].

3. 1. 1. 5. Temperature change

The influence of temperature change on the adsorption capacities of MB dye was reported in Fig. 3A. The results showed that the uptake capacity reduced from 67.7 to 53.9 mg/g (from

90 % to 72% removal) with raising the temperature from 25 to 60°C, suggesting the exothermic nature of the process which may be due to as temperature increase, the physical adsorptive forces between the adsorbed molecules and the adsorbent binding sites are weakened. Furthermore, the dissociation of MB dye also increased and dye–adsorbent interactions decreased [38,42]. The Gibbs free energy, entropy and enthalpy parameters obtained from Van't Hoff's equation [48] and data plotted at Fig. 3B, demonstrated that the adsorption process of MB dye were spontaneous and exothermic as shown in data recorded at table 2.

Fig. (2): Effect of (A) pH, (B) contact time, (C) initial dye concentration and (D) adsorbent dose on the uptake of MB dye using MOF-199.
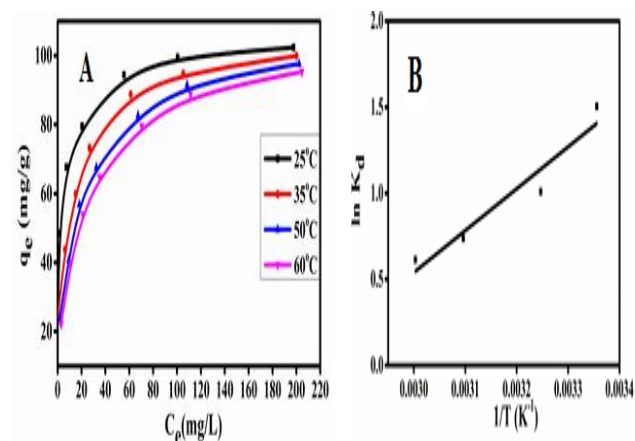
Fig. (3): Effect of temperature on the adsorption of MB over MOF-199 (initial concentration ranging between 25-300 mg/l; contact time 8 h; 50 mg of adsorbent; at 25°C, 35°C, 50°C and 60°C).

Table (2): Thermodynamic parameters for MB dye adsorption using MOF-199 at different temperatures.

K_d				ΔG^o_{ads} (kJ/mol)				ΔH^o_{ads}(kJ/mol)	ΔS^o_{ads}(J/mol.K)
298K	308K	323K	333K	298K	308K	323K	333K	-20.2	-56.2
4.5	2.7	2.1	1.8	-3.45	-2.89	-2.05	-1.49		

3. 2. 2. Adsorption isotherms

For a solid-liquid system, one of the important physico-chemical studies in characterization of sorption behavior is the equilibrium isotherm of sorption which used to characterize the experimental adsorption data. The Langmuir isotherm is the most applied adsorption model and aspects monolayer sorption behavior on the adsorbent surface which contains a homogeneous and definite number of active sites [49,50]. The model

generally expressed in the well-known form represented in the following equation as:

$$q_e = \frac{K_L C_e}{1 + q_m C_e}$$

A linear form of this model expression is

$$\frac{C_e}{q_e} = \frac{1}{K_L q_{max}} + \frac{C_e}{q_{max}}$$

Where C_e (mg/L) is the equilibrium concentration of the adsorbed molecule; q_e (mg/g) is the adsorption capacity of the adsorbent at equilibrium per unit mass of

adsorbent; q_{max} (mg/g) indicates the theoretical sorption capacity and K_L in L/mg is the Langmuir sorption isotherm constant. One of the most important description of the Langmuir isotherm equations is the dimensionless separation factor (R_L), represented in the equation as [51–54]:

$$R_L = \frac{1}{1 + K_L C_o}$$

Where K_L in L/mg is the Langmuir sorption constant and C_o in mg/L is the initial concentration of the adsorbed molecule. The R_L values describe the isotherm type to be either irreversible (R_L=0), linear (R_L=1), unfavorable (R_L>1) or favorable (0<R_L<1). On the other hand, the well-known heterogeneous systems; Freundlich isotherm does not takes into account the formation of monolayer but multilayer and non-ideal adsorption. The Freundlich isotherm model represented by the well-known logarithmic form which expressed in the following equation [51,52] :

$$q_e = K_F C_e^{1/n}$$

A linear form of this expression can be represented as follow:

$$\ln q_e = (1/ n) \ln C_e + \ln K_F$$

Where n (g/L) and K_F ($mg^{1-1/n}L^{1/n}g^{-1}$) are the Freundlich sorption isotherm exponent and constant. K_F describes the adsorption or distribution coefficient giving an indication of the definite quantity of the adsorbed molecule on an adsorbent surface at equilibrium while n indicates the favorability of the sorption isotherm and measure the surface heterogeneity or sorption intensity. The process be more heterogeneous when the value of $1/n$ gets nearer to zero. A value of $1/n$ lower than unity is indicative of Langmuir isotherm while $1/n$ above unity indicating of co-operative sorption [49,51,53]. Langmuir and Freundlich sorption isotherms for MB dye MOF-199 as adsorbent were seen in Fig. 4. The correlation factor coefficients, R^2 and isotherm parameters are calculated and recorded at Table 3. The Langmuir model with R^2 factor of 0.9989, represents accurate fit of the experimental data and more acceptable than that of Freundlich isotherm with R^2 of 0.9619. It gives an indication of the monolayer sorption of MB dye on the homogeneous surface of MOF-199 adsorbent. The maximum monolayer capacity obtained from Langmuir model for the uptake

of MB were found to be 103.5 mg/g. Moreover, the dimensionless separation constant R_L values between 0.0109-0.1173 indicates the favorability of the sorption process for MB dye, also the value of $1/n$ between 0 and 1 also indicates the high sorption intensity as shown at Table 3.

Table (3): The thermodynamic parameters for the adsorption of MB dye using MOF-199.

Langmuir isotherm constants			
K_L(L/g)	q_m(mg/g)	R_L	R^2
0.301	103.51	0.0109-0.1173	0.9989
Freundlich isotherm constants			
K_F (mg/g)	n		R^2
47.7	6.34		0.9619
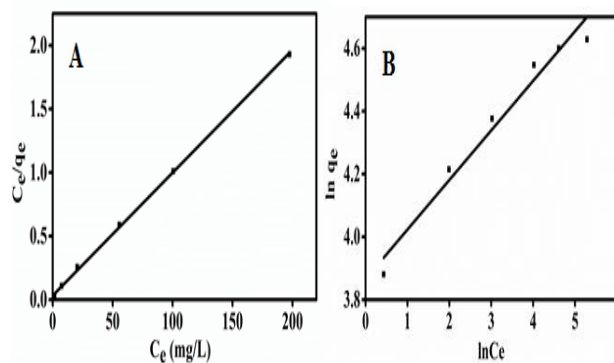
Fig. (4): Langmuir (A) and Freundlich (B) adsorption isotherms (initial concentration 25–300 mg/L for MB , 50 mg adsorbent, 25 °C; at optimum pH).

### 3. 2. 3. Adsorption kinetics

In order to design a plan for adsorption treatment, the rate at which an adsorbate rejected from an aqueous solution is important to be predicted. The two well-known models pseudo 1st order (PFO) and pseudo 2nd order (PSO) [38–40] were applied to the experimental data of the adsorption processes to evaluate the adsorption kinetics. The integrated and linear form of these kinetic models are seen respectively in the following equations:

$$\ln(q_e - q_t) = \ln q_e - k_1 t$$

$$\frac{t}{q_t} = \frac{1}{K_2 q_e^2} + \frac{1}{q_e} t$$

Where k_1 (1/min) and k_2 in g/(mg•min) are respectively the sorption rate constants of the 1st and 2nd pseudo-order; q_e and q_t in mg/g are

respectively the quantities of an adsorbate at equilibrium and time (t). The adsorption kinetic relation plots are seen in Fig. 5 and all the kinetic parameters were calculated and listed at Table 4. The determined R^2 factor for the pseudo 2nd order model is closer to unity than that of pseudo 1st model (0.9992 *vs* 0.9110), therefore these sorption systems follow the pseudo 2nd order kinetic model predominantly.
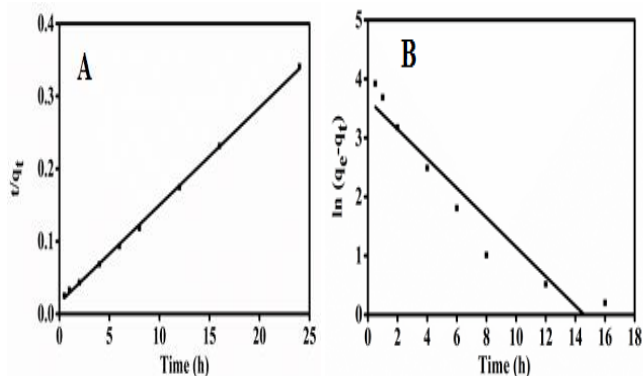
**Fig. (5)**: Pseudo-first (A) and Pseudo-second order (B) kinetic models of MB dye.

Table (4): Kinetic parameters for MB dye using MOF-199 as adsorbent.

1st order model			
k_1 (L/min)	$q_{e,\ calc}$(mg/g)	$q_{e,\ exp}$ (mg/g)	R^2
2.4976	38.36	67.7	0.9110
2nd order model			
k_2 (g/(mg min))	$q_{e,\ calc}$(mg/g)	$q_{e,\ exp}$ (mg/g)	R^2
0.01162	74.4	67.7	0.9992

3. 2. 4. Regeneration of MOF-199

One of the important key factor in water treatment is the reusability (durability) of the adsorbents which are good for the environment from the green chemistry point of view as well as being acceptable to the industry i.e. cost saving and atom economy. Hence, we further examined the durability of MOF-199. In this study, hot ethanol was adopted as the eluent solvent for regeneration of the used adsorbent. As shown in Fig. 6A, MOF-199 almost maintained their initial percent removal (the efficiency decreased only within 5 %) over five repeated runs. From the FT-IR spectral analysis of the 5th reused MOF-199 in comparison with that of fresh one (Fig. 6B), there is no obvious change happened to groups of MOF-199 during its recovering i.e. showed the same spectral peaks. In conclusion, MOF-199 adsorbent was easily recovered after the dye uptake process and reused at least five times.
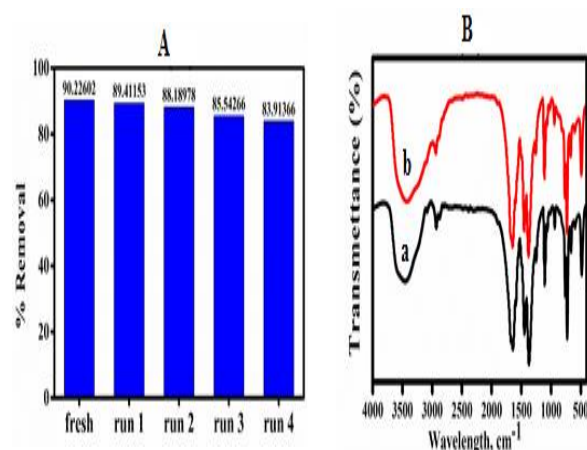
Fig. (6): (A) Reusability of MB using MOF-199 and **(B)** FT-IR of (a) fresh and (b) reused MOF-199

Conclusion

MOF-199 adsorbent was prepared successfully and characterized using FT-IR and SEM. The adsorption study of MB using MOF-199 indicated that the removal efficiency has been reached closely 100% at lower initial concentration (25, 50 mg/l) with fast kinetics, but in case of higher concentration of MB, the efficiency of MOF-199 was reduced around 50% of the original value. The adsorption performance has been greatly improved at pH 10 with removal efficiency reached approximately 90% from 75 mg/l of MB dye solution and the adsorption equilibrium on the prepared material was reached after 8h under optimum conditions. The study of temperature change demonstrates that the sorption efficiency decreased with increasing temperature from 25 to 60°C suggesting the exothermic nature of the sorption process. The experimental data resulted from the equilibrium studies were fitted to Langmuir sorption model more than Freundlich and this adsorption system follows the pseudo 2nd order kinetic model further than pseudo 1st order. The FT-IR spectral analysis confirmed the good reusability and high structure stability of the adsorbent and the results showed that even after the 5th run, MOF-199 still well maintained nearly the initial adsorptive removal. Subsequently, we trust that MOF-199 composite as an adsorbent can have a

promising future for environmental pollutants purification and separation.

4. References

1   A. Lajevardi, M.T. Yaraki, A. Masjedi, A. Nouri, M.H. Sadr, (2018) *J. Mol. Liq.* #pagerange#.

2   O.M. Yaghi, M. O'Keeffe, N.W. Ockwig, H.K. Chae, M. Eddaoudi, (2003) *J. Kim, Nature* **423** 705–714.

3   A.C. Functionalizable, N. Material, C. Tma, S.S. Chui, S.M. Lo, J.P.H. Charmant, A.G. Orpen, I.D. Williams, C.T.M.A. Ho, S.S. Chui, S.M. Lo, J.P.H. Charmant, A.G. Orpen, I.D. (2016)Williamsl, 283 1148–1150.

4   O.M. Yaghi, 7863 (1998) 1–2.

5   K.J.H.J.R. Ridd, J.C. Soc, P. Trans, T.G. Traylor, A.R. Miksztal, J.A.C. Soc, O.B.J.O. Gradv, F.N.M.J. Am, C. Soc, M. Newcomb, Angew. (1997) Chem. Int. Ed. **36** 1725–1727.

6   H. Furukawa, K.E. Cordova, M. O'Keeffe, O.M. Yaghi, (2013).Science (80-.). 341

7   M. Eddaoudi, J. Kim, N. Rosi, D. Vodak, J. Wachter, M.O. Keeffe, O.M. Yaghi, M. Eddaoudi, J. Kimrn, N. Rosi, O.M. Yaghil(2016), **295** 469–472.

8   T.R. Zeitler, M.D. Allendorf, J.A. Greathouse, (2012) *J. Phys. Chem. C* **116** 3492–3502.

9   O.K. Farha, C.E. Wilmer, I. Eryazici, B.G. Hauser, P.A. Parilla, K. ONeill, A.A. Sarjeant, S.T. Nguyen, R.Q. Snurr, J.T. Hupp, (2012) *J. Am. Chem. Soc.* **134** 9860–9863.

10 K. Koh, A.G. Wong-Foy, A.J. Matzger, J. Am. (2009)Chem. Soc. **131** 4184–4185.

11 M. Eddaoudi, M. Eddaoudi, J. Kim, N. Rosi, O.M. Yaghi, **469** (2012) 32–34.

12 K.S. Park, Z. Ni, A.P. Cote, J.Y. Choi, R. Huang, F.J. Uribe-Romo, H.K. Chae, M. O'Keeffe, O.M. Yaghi, (2006) Proc. Natl. Acad. Sci. **103** 10186–10191.

13 J.H. Cavka, S. Jakobsen, U. Olsbye, N. Guillou, S. Bordiga, K.P. Lillerud, C. Lamberti, S. Bordiga, K.P. Lillerud, (2008) *J. Am. Chem. Soc*. **130** 1–19.

14 M. Kandiah, M.H. Nilsen, S. Usseglio, S. Jakobsen, U. Olsbye, M. Tilset, C. Larabi, E.A. Quadrelli, F. Bonino, K.P. Lillerud, (2010)Chem. Mater. **22** 6632–6640.

15 U. Mueller, M. Schubert, F. Teich, H. Puetter, K. Schierle-Arndt, J. Pastré, (2006)*J. Mater. Chem.* **16** 626–636.

16 M. Elimelech, B.J. Marinas, M.A. Shannon, P.W. Bohn, J.G. Georgiadis, A.M. Mayes, (2008)Nature **452** 301–310.

[17 C.J. Vörösmarty, P. Green, J. Salisbury, B. Richard, C.J. Vorosmarty, P. Green, J. Salisbury, R.B. (2016) Lammers, **289** 284–288.

18 C.J. Vörösmarty, P.B. McIntyre, M.O. Gessner, D. Dudgeon, A. Prusevich, P. Green, S. Glidden, S.E. Bunn, C.A. Sullivan, C.R. Liermann, P.M. Davies, (2010)Nature 468 334.

19 J. Yeston, R. Coontz, J. Smith, C. Ash, (2006)Science (80-.). 313 1067.

20 J.G.B. Derraik, Mar. (2002) Pollut. Bull. **44** 842–852.

21 F. Wang, Z.S. Liu, H. Yang, Y.X. Tan, J. Zhang, Angew. (2011) Chemie - Int. Ed. 50 450–453.

22 A.K. Ghattas, F. Fischer, A. Wick, T.A. Ternes, (2017)Water Res. **116** 268–295.

23 C. Grandclément, I. Seyssiecq, A. Piram, P. Wong-Wah-Chung, G. Vanot, N. Tiliacos, N. Roche, P. Doumenq, (2017) Water Res. **111** 297–317.

24 G. Zelmanov, R. Semiat, (2008)Water Res. **42** 492–498.

25 G. Xu, X. Zhang, P. Guo, C. Pan, H. Zhang, C. Wang, (2010)*J. Am. Chem. Soc*. **132** 3656–3657.

26 Y.L. Pang, A.Z. Abdullah, S. Bhatia, (2011)Desalination **277** 1–14.

27 J.Q. Jiang, N. Graham, C. André, G.H. Kelsall, N. Brandon, (2002) Water Res. **36** 4064–4078.

28 G. Montes-Hernandez, N. Concha-Lozano, F. Renard, E. Quirico, (2009)*J. Hazard. Mater*. **166** 788–795.

29 A. Erto, F.E. Soetaredjo, B. Ernst, (2018) *J. Mol. Liq. #pagerange#.*

30 A. Loudet, K. Burgess, Am. (2007) Chem. Soc. **107** 4891–4932.

31 S. Pang, Y. Wu, X. Zhang, B. Li, J. Ouyang, M. Ding, (2015).Process Biochem.

32 L.T.L. Nguyen, T.T. Nguyen, K.D. Nguyen, N.T.S. Phan, Appl. (2012) Catal. A Gen. 425–426 44–52.

33 D. Britt, D. Tranchemontagne, O.M.

Yaghi, Proc. (2008) Natl. Acad. Sci. **105** 11623–11627.

34 S. Marx, W. Kleist, A. Baiker, (2011) *J. Catal.* **281** 76–87.

35 X. Fang, Y. Shi, K. Wu, J. Liang, Y. Wu, M. Yang, RSC Adv. **7** (2017) 40581–40590.

36 A. Gupta, C. Balomajumder, Appl. Water Sci. **7** (2017) 4361–4374.

37 K.A. Shroff, V.K. Vaidya, *Chem. Eng. J.* **171** (2011) 1234–1245.

38 E. Haque, V. Lo, A.I. Minett, A.T. Harris, T.L. Church, *J. Mater. Chem. A* 2 (2014) 193–203.

39 J.O. Babalola, F.T. Olayiwola, J.O. Olowoyo, A.H. Alabi, E.I. Unuabonah, A.E. Ofomaja, M.O. Omorogie, *Int. J. Ind. Chem.* **8** (2017) 207–220.

40 Z. Hasan, S.H. Jhung, J. Hazard. Mater. **283** (2015) 329–339.

41 I. Ahmed, S.H. Jhung, Mater. Today **17** (2014) 136–146.

42 X.-X. Huang, L.-G. Qiu, W. Zhang, Y.-P. Yuan, X. Jiang, A.-J. Xie, Y.-H. Shen, J.-F. Zhu, CrystEngComm **14** (2012) 1613–1617.

43 H.-N. Wang, F.-H. Liu, X.-L. Wang, K.-Z. Shao, Z.-M. Su, *J. Mater. Chem. A 1* (2013) 13060.

44 L. Xie, D. Liu, H. Huang, Q. Yang, C. Zhong, *Chem. Eng. J.* **246** (2014) 142–149.

45 A. Kausar, M. Iqbal, A. Javed, K. Aftab, Z. i. H. Nazli, H.N. Bhatti, S. Nouren, *J. Mol. Liq.* **256** (2018) 395–407.

46 M. Mushtaq, H.N. Bhatti, M. Iqbal, S. Noreen, *J. Environ. Manage.* **176** (2016) 21–33.

47 Q. Manzoor, R. Nadeem, M. Iqbal, R. Saeed, T.M. Ansari, Bioresour. Technol. **132** (2013) 446–452.

48 E.C. Lima, A. Hosseini-bandegharaei, J.C. Moreno-piraján, I. Anastopoulos, *J. Mol. Liq.* **273** (2019) 425–434.

49 P.T. Dhorabe, D.H. Lataye, R.S. Ingole, J. Hazardous, Toxic, Radioact. Waste 21 (2017) 04016015.

50 C. Gerente, V.K.C. Lee, P. Le Cloirec, G. McKay, Crit. Rev. Environ. Sci. Technol. **37** (2007) 41–127.

51 Ö. Demirbaş, M. Alkan, Desalin. Water Treat. **53** (2015) 3623–3631.

52 B. Das, N.K. Mondal, R. Bhaumik, P. Roy, *Int. J. Environ. Sci. Technol.* 11 (2014) 1101–1114.

53 N. Boudechiche, H. Mokaddem, Z. Sadaoui, M. Trari, I*nt. J. Ind. Chem.* **7** (2016) 167–180.

54 L. Wang, J. Zhang, A. Wang, Colloids Surfaces A Physicochem. Eng. Asp. **322** (2008) 47–53.